

## Electronic Supplementary Information

### Non-enzymatic glucose sensor based on mesoporous carbon sphere immobilized Co-MOF-74 nanocomposite

Xianliang Li,<sup>a\*</sup> Diwei Deng,<sup>a</sup> Lufang He,<sup>b</sup> Yan Xu,<sup>b</sup>

<sup>a</sup>College of Materials Science and Engineering, Shenyang University of Chemical Technology, Shenyang, Liaoning 110142, China. \*E-mail: lixianliang007@163.com (Xianliang Li).

<sup>b</sup>Department of Chemistry, College of Sciences, Northeastern University, Shenyang, Liaoning 110819, PR China.

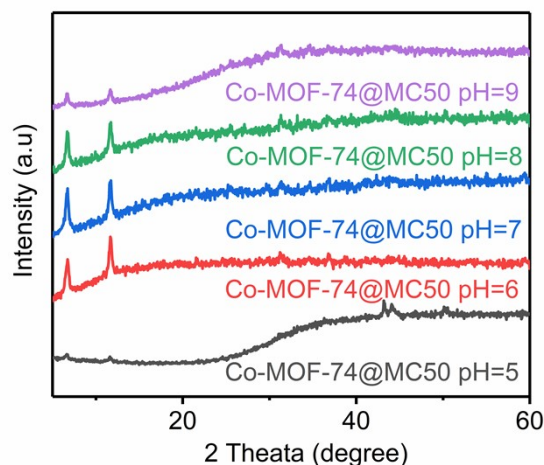


**Fig. S1** Chemical stability of Co-MOF-74/MC-50 nanocomposite in aqueous solution at different pH.

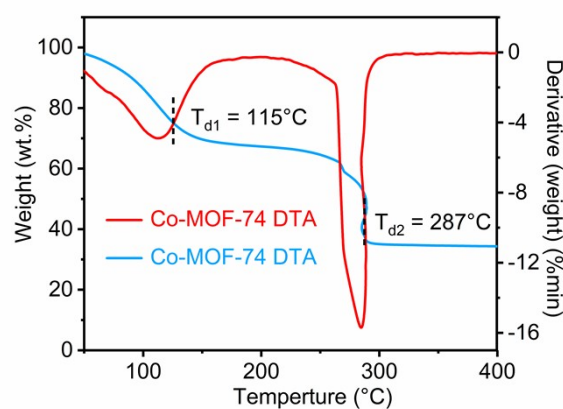


**Fig. S2** Thermal stability of Co-MOF-74 characterized by thermogravimetric-differential thermal analysis (TG-DTA).

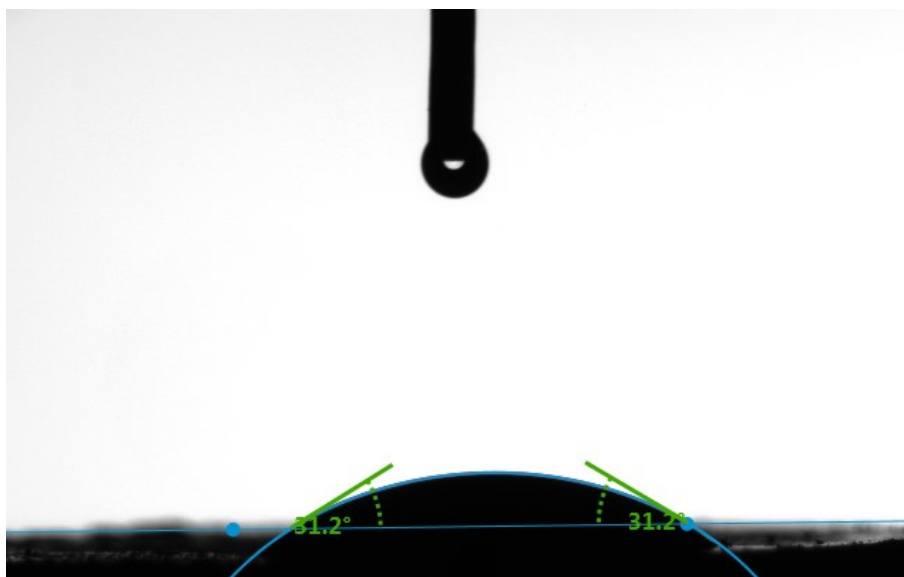


**Fig. S3** Contact angle of pure Co-MOF-74 crystals.

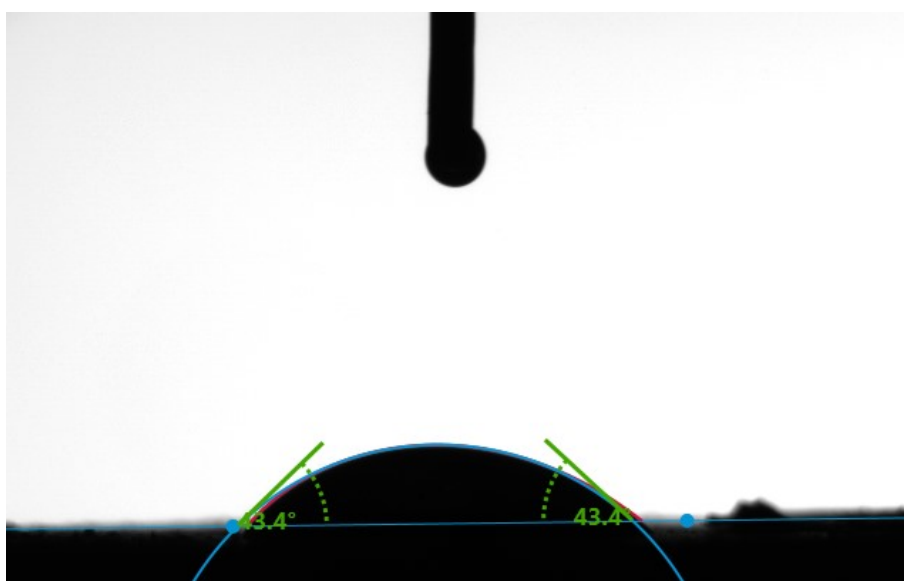


**Fig. S4** Contact angle of Co-MOF-74/MC-50 nanocomposite.

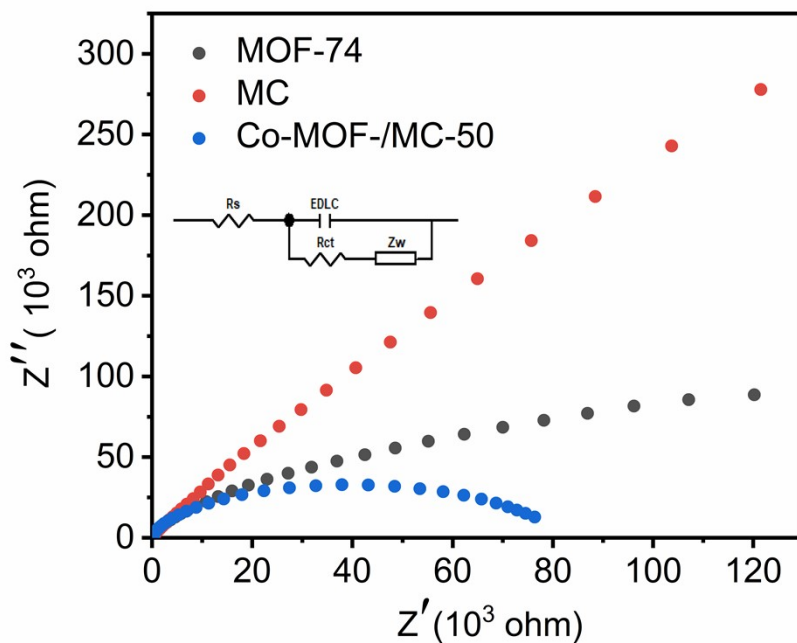


**Fig. S5** EIS spectra of the corresponding MC, MOF-74, and Co-MOF-74/MC-50 modified GCE electrodes, inset: fitted equivalent circuit diagram obtained by Z-view software fitting ( $R_s$  is the electrolyte resistance,  $R_{ct}$  is the charge transfer resistance, and  $Z_w$  is the Warburg impedance).

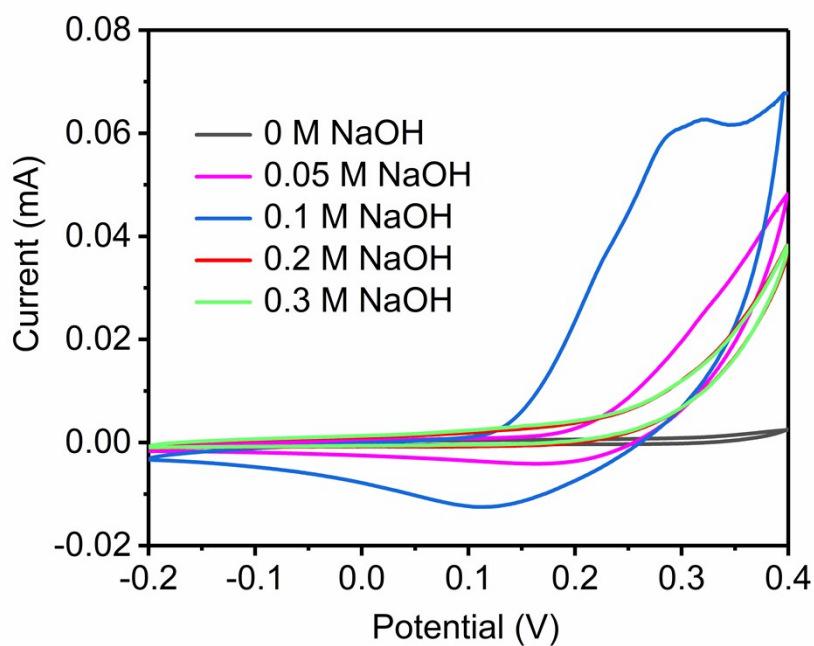


**Fig. S6** CV curves of Co-MOF-74/MC-50 modified GCE electrode recorded in NaOH solution with different concentrations containing 10 mM glucose.

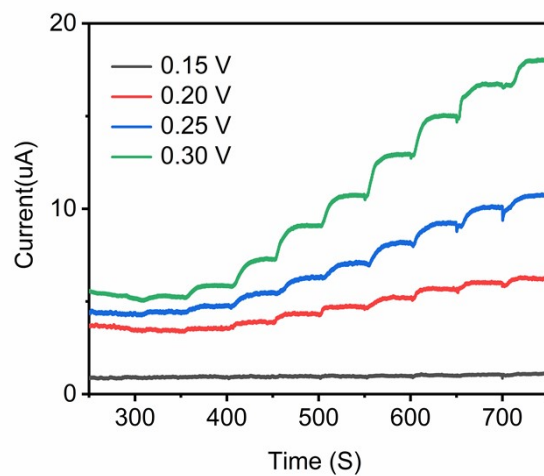


**Fig. S7** I-T curves of Co-MOF-74/MC-50 modified GCE electrode towards glucose at different operating potentials (0.15-0.30 V).

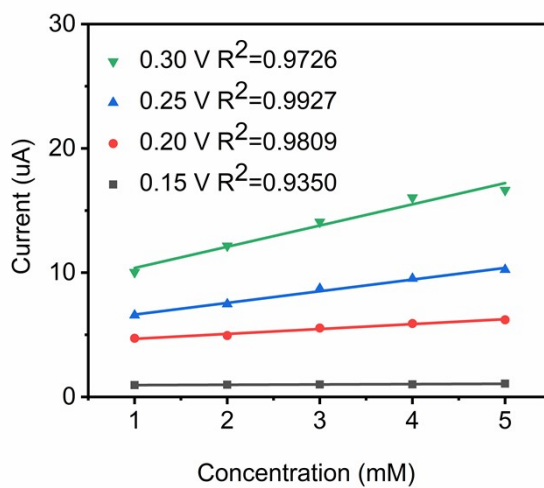


**Fig. S8** The calibration curves of glucose concentration versus current signals.